

# Analysis of the reverse leakage current in AlGaIn/GaN Schottky barrier diodes treated with fluorine plasma

Woo Jin Ha,<sup>1</sup> Sameer Chhajed,<sup>1</sup> Seung Jae Oh,<sup>1</sup> Sunyong Hwang,<sup>1</sup> Jong Kyu Kim,<sup>1,a)</sup> Jae-Hoon Lee,<sup>2</sup> and Ki-Se Kim<sup>2</sup>

<sup>1</sup>Department of Materials Science and Engineering, Pohang University of Science and Technology (POSTECH), Pohang 790-784, South Korea

<sup>2</sup>Samsung LED Co., Ltd., Suwon 443-743, South Korea

(Received 23 February 2012; accepted 7 March 2012; published online 27 March 2012)

The carrier transport mechanism of CF<sub>4</sub> plasma-treated AlGaIn/GaN Schottky barrier diodes (SBDs) under reverse bias is investigated. The reverse leakage current is reduced by ~2 orders of magnitude after the CF<sub>4</sub> plasma treatment, but increases exponentially with increasing temperature, indicating that a thermally activated transport mechanism is involved. Based on the activation energy estimated from temperature-dependent current-voltage characteristics and the emission barrier height extracted from Frenkel-Poole emission model, it is suggested that the dominant carrier transport mechanism in the CF<sub>4</sub> plasma treated SBDs is the Frenkel-Poole emission from fluorine-related deep-level states into the continuum states of dislocations. © 2012 American Institute of Physics. [<http://dx.doi.org/10.1063/1.3697684>]

A large reverse leakage current in AlGaIn/GaN-based electronic devices such as high electron mobility transistors (HEMTs) and Schottky barrier diodes (SBDs) remains a big hurdle in development of high power and high frequency devices.<sup>1</sup> Several methods have been proposed to reduce reverse leakage current, including O<sub>2</sub> or N<sub>2</sub>-based plasma treatments, passivation of AlGaIn surface using SiN<sub>x</sub> or SiO<sub>2</sub>, and adding dielectric layers such as Al<sub>2</sub>O<sub>3</sub> and HfO<sub>2</sub> between the Schottky metal and the AlGaIn layer.<sup>2-7</sup>

Recently, it was found that surface treatments using fluorine-based plasma using C<sub>2</sub>F<sub>6</sub> or CF<sub>4</sub> can effectively reduce the leakage current of the Schottky contacts on AlGaIn/GaN heterostructures. Chu *et al.* have reported a large reduction in reverse leakage current by CF<sub>4</sub> plasma treatment.<sup>8</sup> Furthermore, the fluorine plasma treatment has been demonstrated to shift the threshold voltage of AlGaIn/GaN HEMTs toward a positive value,<sup>9</sup> enabling the enhancement-mode operation.<sup>10-12</sup> Although a number of studies regarding the performance of fluorine-plasma-treated AlGaIn/GaN-based devices have been done, more systematic characterization and a more detailed understandings of the relevant mechanism of carrier transport under reverse bias are of fundamental importance to further improve the device performance.

In this study, we have analyzed the evolution of chemical bonding states at the AlGaIn surface treated with CF<sub>4</sub> plasma and corresponding changes in temperature-dependent electrical characteristics of AlGaIn/GaN SBDs. Based on these results, the dominant carrier transport mechanism of the CF<sub>4</sub> plasma-treated AlGaIn/GaN under reverse biases is suggested.

The AlGaIn/GaN SBD structures were grown on c-plane sapphire substrates using metal organic chemical vapor deposition. Trimethylgallium (TMGa), trimethylaluminum (TMAI), and ammonia (NH<sub>3</sub>) were used as precursors for GaN and AlGaIn growth. The SBD structure consists of a

30 nm GaN nucleation layer, followed by a 3 μm highly resistive GaN buffer layer, a 1 nm AlN interfacial layer, and a 35 nm AlGaIn barrier layer with an Al mole fraction of 15%. For isolating each device, mesa structures on which both ohmic and Schottky contacts are deposited were fabricated by inductively coupled plasma etching using a Cl<sub>2</sub>/BCl<sub>3</sub> chemistry. Ti/Al/Ni/Au (30/120/40/50 nm) ohmic contacts were deposited by electron-beam evaporation followed by a rapid thermal annealing at 750 °C for 1 min in nitrogen ambient. The specific contact resistivity of  $7.9 \times 10^{-5} \Omega\cdot\text{cm}^2$  and the sheet resistance of 602 Ω were obtained by the transfer length method. After the ohmic contact formation, a reactive ion etching system was used for the CF<sub>4</sub> plasma treatment on whole wafer surface at various radio frequency (RF) powers of 50 W, 100 W, and 300 W for 1 min under the CF<sub>4</sub> gas flow of 10 sccm, and the operating pressure of 3 mTorr. After the CF<sub>4</sub> plasma treatments, Ni/Au (200/200 nm) Schottky contacts were deposited on the plasma treated mesa surface using electron-beam evaporation. The current-voltage (*I*-*V*) characteristics were measured at various temperatures from 298 K up to 473 K. The chemical bonding states of the AlGaIn surfaces with and without CF<sub>4</sub> plasma treatments were characterized by synchrotron radiation photoemission spectroscopy (SRPES) using the 24A1 beamline at the Taiwan Photon Source. Ga 3*d*, N 1*s*, O 1*s*, C 1*s*, Al 2*p*, and F 1*s* core-level spectra together with Au 4*f* for binding energy calibration were obtained.

Figure 1 shows the *I*-*V* characteristics of the reference and the AlGaIn/GaN SBDs with CF<sub>4</sub> plasma treatment at RF powers of 50 W and 100 W. The reverse leakage current decreases to 1/3 of its original value with the 50 W RF plasma treatment and further decreases by nearly two orders of magnitude with the 100 W RF plasma treatment. As RF plasma power increases, the ideality factor decreases from 1.19 (reference) to 1.10 (100 W-treated), and the forward current, as shown in the inset of Fig. 1, decreases slightly possibly due to the depletion of 2 dimensional electron gas (2DEG). Cai *et al.* proposed that fluorine atoms incorporated

<sup>a)</sup>Electronic mail: kimjk@postech.ac.kr.

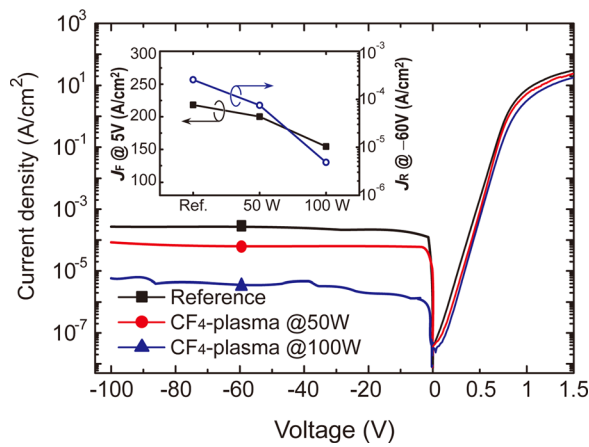


FIG. 1. The  $I$ - $V$  characteristics of the AlGaIn/GaN Schottky barrier diodes with and without  $\text{CF}_4$  plasma treatments at RF plasma power of 50 W and 100 W. The inset shows the forward current density  $J_F$  at 5 V and the reverse leakage current density  $J_R$  at  $-60$  V for each sample.

into the AlGaIn barrier layer during the  $\text{CF}_4$  plasma treatment form immobile negative charges due to the strong electronegativity of the fluorine ions, resulting in the depletion of the 2DEG at the interface of AlGaIn/GaN heterostructure.<sup>10</sup> Further increase in the RF power up to 300 W results in the increase of reverse leakage current as well as significant decrease of the forward current.

In order to investigate the origin of the reduction of reverse leakage current, SRPES was carried out on the AlGaIn surfaces with and without the  $\text{CF}_4$  plasma treatments. The Ga 3d, N 1s, O 1s, core-level spectra do not show a noticeable change in shape and intensity, whereas the F 1s and C 1s spectra do, as shown in Fig. 2. It is clearly seen that the F 1s core-level spectra appear after the  $\text{CF}_4$  plasma treatments, indicating that fluorine atoms were incorporated near the surface of AlGaIn layer during the plasma treatments. Taken together with the  $I$ - $V$  characteristics shown in Fig. 1, the reduction of reverse leakage current is closely related to the surface modification by the incorporation of fluorine atoms. For the device treated with RF power of 50 W, high intensity F 1s spectrum appears, and the C 1s spectrum

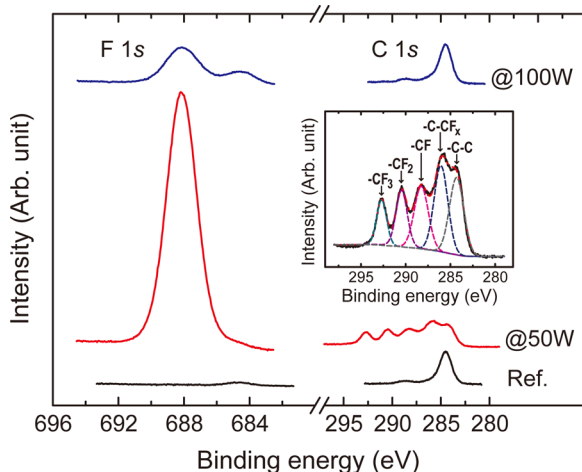


FIG. 2. The SRPES spectra of F 1s and C 1s core-levels from the AlGaIn surface with and without  $\text{CF}_4$  plasma treatment. The inset shows the spectral deconvolution of C 1s spectrum of the plasma-treated sample at RF power of 50 W.

seems to be a combination of several peaks. Spectral deconvolution of the C 1s spectrum reveals that it consists of five components,  $-\text{CF}_3$ ,  $-\text{CF}_2$ ,  $-\text{CF}$ ,  $-\text{C}-\text{CF}_x$ , and  $-\text{C}-\text{C}$  bonds, as shown in the inset of Fig. 2.<sup>13</sup> Together with the large F 1s spectrum, the deconvolution result indicates that  $\text{CF}_4$  gas was not fully decomposed at RF plasma power of 50 W and adsorbed predominantly at the surface of the AlGaIn layer in forms of several radicals as indicated in the inset. No significant change in core level spectra, not shown here, other than the F 1s spectrum between the reference and the 100 W-treated sample indicates that there is no remarkable chemical reaction except for the incorporation of fluorine atoms. For the sample treated at RF plasma power of 300 W, the appearance of a new peak with the binding energy of 76.5 eV was observed indicating the formation of  $\text{AlF}_3$  layer at the AlGaIn surface.

In order to investigate the change in carrier transport mechanism by the  $\text{CF}_4$  plasma treatments, temperature-dependent  $I$ - $V$  characteristics were measured with elevating temperature from 298 K to 473 K. Figure 3 shows the reverse leakage current density at  $-60$  V as a function of temperature for the reference and the plasma-treated SBDs at RF powers of 50 W and 100 W. The reverse leakage current of the reference shows an unusual behavior, i.e., it decreases by 2.5 times when the temperature increases from room temperature to 473 K, which is still not fully understood at the moment and further investigation is needed. The 50 W-treated SBD shows negligible temperature-dependent reverse leakage current, indicating that tunneling is the dominant transport mechanism. On the other hand, the reverse leakage current in the plasma-treated sample at RF power of 100 W increases exponentially with increasing temperature, and it becomes larger than that of the other samples above  $\sim 440$  K. This implies that a thermally activated transport mechanism becomes dominant when the fluorine atoms are incorporated at the AlGaIn surface. The 100 W-plasma-treated SBD exhibits the linear region in the Arrhenius plot, suggesting that a thermally activated mechanism with an  $\exp(-E_A/kT)$  functional dependence where  $E_A$  is an activation energy

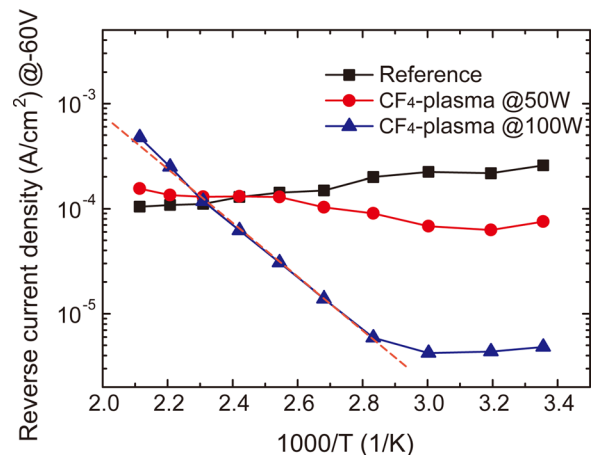


FIG. 3. The reverse leakage current density at  $-60$  V as a function of temperature for the SBDs with and without  $\text{CF}_4$  plasma treatments. The activation energy of 0.63 eV is estimated from the linear fit (dotted line) for the plasma treated sample at RF power of 100 W.

becomes dominant. From the linear fit indicated by the dotted line, the activation energy is estimated to be 0.63 eV.

Next, we investigated the possible origin of the thermally activated transport mechanism with the activation energy of  $\sim 0.63$  eV responsible for the large change in the temperature-dependent  $I$ - $V$  characteristics induced by the plasma treatment. Among several possibilities evaluated, a transport model based on Frenkel-Poole emission satisfies our measured data with acceptable values of the physical parameters.<sup>14</sup> The Frenkel-Poole emission is a trap-mediated transport mechanism where the carrier density depends exponentially on the activation energy of the traps that is corrected for the electric field so that the current density is given by<sup>14-16</sup>

$$J = CE_b \exp \left[ -\frac{q(\phi_t - \sqrt{qE_b/\pi\epsilon_0\epsilon_s})}{kT} \right], \quad (1)$$

where  $J$  is the current density,  $E_b$  is the electric field in the AlGaIn barrier,  $\phi_t$  is the barrier height for electron emission from a trap state,  $\epsilon_s$  is the high-frequency relative dielectric permittivity,  $\epsilon_0$  is the permittivity of free space, and  $k$  is Boltzmann's constant. From Eq. (1),  $\log(J/E_b)$  is a linear function of  $\sqrt{E_b}$ , i.e.,

$$\log \left( \frac{J}{E_b} \right) = \frac{q}{kT} \sqrt{\frac{qE_b}{\pi\epsilon_0\epsilon_s}} - \frac{q\phi_t}{kT} + \log C \equiv m(T)\sqrt{E_b} + b(T). \quad (2)$$

Figure 4(a) shows the plot of  $J/E_b$  with logarithmic scale as a function of square root of  $E_b$  for the 100 W-plasma-treated SBDs with increasing temperature. Figure 4(b) shows the temperature-dependent slope,  $m(T)$ , and intercept,  $b(T)$ . Both  $m(T)$  and  $b(T)$  are linear functions against inverse temperature, which is expected in Frenkel-Poole emission model. The dielectric constant  $\epsilon_s$  and the emission barrier height  $\phi_t$  for the plasma-treated sample extracted from Fig. 4(b) and Eq. (2) are  $\epsilon_s = 4.85$  and  $\phi_t = 0.65$  eV. Note that the high-frequency (optical) dielectric constant, rather than the static one, should be used in the Frenkel-Poole model<sup>14</sup> due to much faster trap emission process ( $10^{-14}$ – $10^{-15}$  s)<sup>17</sup> than the dielectric relaxation time ( $10^{-11}$ – $10^{-13}$  s), therefore, there is little or no polarization response from the surrounding atoms. The value of  $\epsilon_s$  is in good agreement with the reported values of 5.35 for GaN and 4.77 for AlN<sup>18</sup> and the activation energy of 0.63 eV estimated from Arrhenius plot in Fig. 3, further supporting the validity of Frenkel-Poole emission model in describing the current transport mechanism with reasonable physical parameters.

Frenkel-Poole emission model describes an electric-field-enhanced emission from a trap state into typically, but not necessarily, the conduction band. Given experimentally determined values of the emission barrier height (0.65 eV) and the activation energy (0.63 eV), it is unlikely that the transport mechanism governing the reverse leakage current for the 100 W-treated SBDs is the emission of carriers from a trap state into the conduction band since there is no reported trap state with activation energy of  $\sim 0.6$  eV from the conduction band. However, a modified Frenkel-Poole emission from a trap state into a continuum of states, possibly associated with

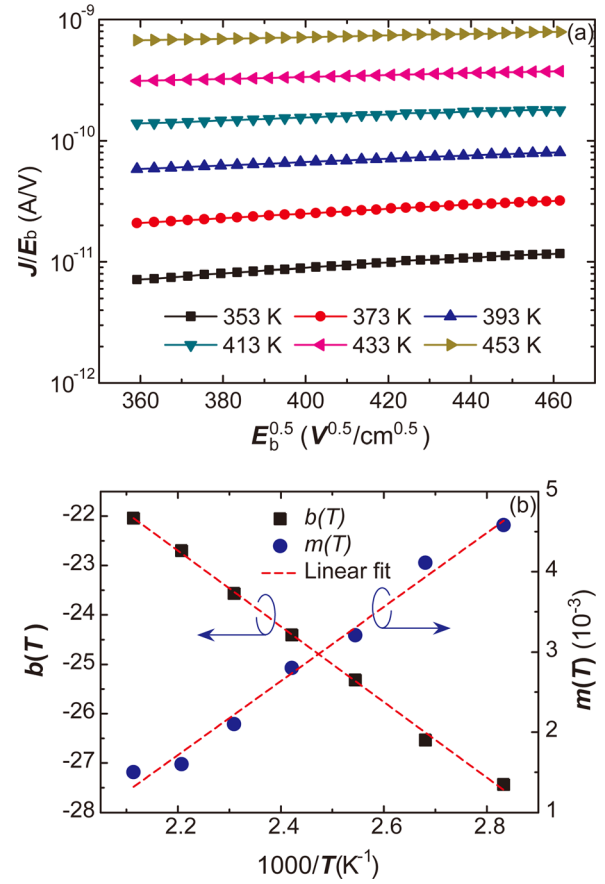


FIG. 4. (a) Measured current density divided by the electric field in the AlGaIn barrier  $E_b$  versus square root of the  $E_b$  for the plasma-treated sample at RF power of 100 W. (b) The intercept  $b(T)$  and the slope  $m(T)$  of the curves shown in (a) as a function of temperature.

conductive dislocations as suggested by Zhang *et al.*,<sup>19</sup> is a likely postulate, which requires the energy difference of  $\sim 0.6$  eV between the two states. Several studies have shown that conduction associated with threading screw dislocations, which exist in high concentrations in GaN-based semiconductors forming trap states with activation energy of  $\sim 0.9$  eV,<sup>20</sup> is the dominant source of high leakage current at room temperature.<sup>21-23</sup> In addition, the thermal activation energy of fluorine-related deep trap state formed by fluorine-based plasma treatments was estimated to be about 1.5 eV.<sup>24</sup> Based on these reports and our analysis results, we suggest that the dominant reverse leakage current transport mechanism in the  $CF_4$  plasma treated SBDs is the Frenkel-Poole emission from fluorine-related deep-level states (located near 1.5 eV below the conduction band) into the continuum states of conducting dislocations (with the activation energy of  $\sim 0.9$  eV), as schematically shown in Fig. 5.

In summary, the carrier transport mechanism of Schottky contacts on the AlGaIn/GaN SBDs with  $CF_4$  plasma treatments is investigated. The reverse leakage current is reduced by 2 orders of magnitude after the  $CF_4$  plasma treatment with RF power of 100 W due to the incorporation of fluorine atoms in the AlGaIn surface as revealed by the SRPES analysis, lifting the conduction band of AlGaIn near the interface with the Schottky contact. However, while the reverse leakage current of the reference SBD shows temperature-invariant characteristics, that of the 100 W-plasma-treated devices increases

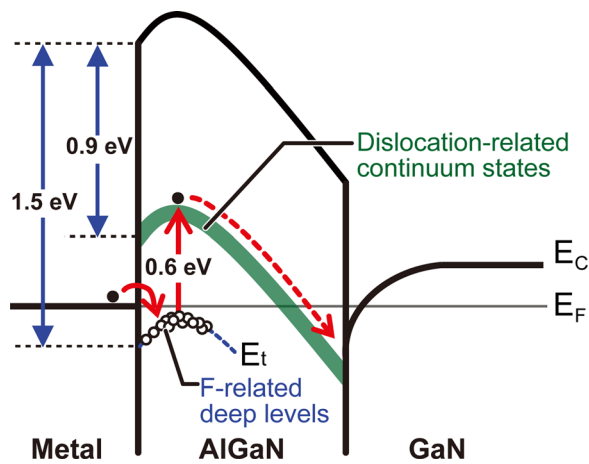


FIG. 5. A schematic energy band diagram showing the proposed Frenkel-Poole emission mechanism in the SBDs with  $\text{CF}_4$  plasma treatment at RF power of 100 W.

exponentially with increasing temperature, suggesting a thermally activated transport mechanism with the activation energy of  $\sim 0.63$  eV is involved. Frenkel-Poole emission model satisfies our measured temperature-dependent relation between the current density and the electric field at AlGaN layer with acceptable values of the physical parameters. Based on these results, it is suggested that the dominant carrier transport mechanism in the  $\text{CF}_4$  plasma treated device under elevated temperature is the Frenkel-Poole emission from fluorine-related deep-level states into the conducting dislocation-related states.

The authors gratefully acknowledge support by the Industrial Technology Development Program funded by Korean Ministry of Knowledge Economy and Basic Science Research Program and Priority Research Centers Program through the National Research Foundation of Korea (NRF) funded by the Ministry of Education, Science and Technology (4.0006850.01, 2010-0029711).

- <sup>1</sup>J. Kotani, S. Kasai, T. Hashizume, and H. Hasegawa, *J. Vac. Sci. Technol. B* **23**, 1799 (2005).
- <sup>2</sup>T. Hashizume, S. Ootomo, S. Oyama, M. Konishi, and H. Hasegawa, *J. Vac. Sci. Technol. B* **19**, 1675 (2001).
- <sup>3</sup>J. H. Kim, H. G. Choi, M.-W. Ha, H. J. Song, C. H. Roh, J. H. Lee, J. H. Park, and C.-K. Hahn, *Jpn. J. Appl. Phys.* **49**, 04DF05 (2010).
- <sup>4</sup>A. Motayed, A. Sharma, K. A. Jones, M. A. Derenge, A. A. Iliadis, and S. N. Mohammad, *J. Appl. Phys.* **96**, 3286 (2004).
- <sup>5</sup>R. Dimitrov, V. Tilak, W. Yeo, B. Green, H. Kim, J. Smart, E. Chumbes, J. R. Shealy, W. Schaff, L. F. Eastman, C. Miskys, O. Ambacher, and M. Stutzmann, *Solid-State Electron.* **44**, 1361 (2000).
- <sup>6</sup>T. Hashizume, S. Ootomo, T. Inagaki, and H. Hasegawa, *J. Vac. Sci. Technol. B* **21**, 1828 (2003).
- <sup>7</sup>T. Hashizume, S. Anantathanasarn, N. Negoro, E. Sano, H. Hasegawa, K. Kumakura, and T. Makimoto, *Jpn. J. Appl. Phys.* **43**, L777 (2004).
- <sup>8</sup>R. Chu, C. S. Suh, M. H. Wong, N. Fichtenbaum, D. Brown, L. McCarthy, S. Keller, F. Wu, J. S. Speck, and U. K. Mishra, *IEEE Electron Device Lett.* **28**, 781 (2007).
- <sup>9</sup>Y. Cai, Y. Zhou, K. M. Lau, and K. J. Chen, *IEEE Trans. Electron Devices* **53**, 2207 (2006).
- <sup>10</sup>Y. Cai, Y. Zhou, K. J. Chen, and K. M. Lau, *IEEE Electron Device Lett.* **26**, 435 (2005).
- <sup>11</sup>T. Palacios, C.-S. Suh, A. Chakraborty, S. Keller, S. P. DenBaars, and U. K. Mishra, *IEEE Electron Device Lett.* **27**, 428 (2006).
- <sup>12</sup>G. Greco, F. Giannazzo, A. Frazzetto, V. Raineri, and F. Roccaforte, *Nanoscale Res. Lett.* **6**, 132 (2011).
- <sup>13</sup>K. Takahashi, M. Hori, and T. Goto, *J. Vac. Sci. Technol. A* **14**, 2004 (1996).
- <sup>14</sup>J. Frenkel, *Phys. Rev.* **54**, 647 (1938).
- <sup>15</sup>J. R. Yeagan and H. L. Taylor, *J. Appl. Phys.* **39**, 5600 (1968).
- <sup>16</sup>J. G. Simmons, *Phys. Rev.* **155**, 657 (1967).
- <sup>17</sup>D. S. Jeong, H. B. Park, and C. S. Hwang, *Appl. Phys. Lett.* **86**, 072903 (2005).
- <sup>18</sup>V. W. L. Chin, T. L. Tansley, and T. Osotchan, *J. Appl. Phys.* **75**, 7365 (1994).
- <sup>19</sup>H. Zhang, E. J. Miller, and E. T. Yu, *J. Appl. Phys.* **99**, 023703 (2006).
- <sup>20</sup>A. Hierro, A. R. Arehart, B. Heying, M. Hansen, U. K. Mishra, S. P. DenBaars, J. S. Speck, and S. A. Ringel, *Appl. Phys. Lett.* **80**, 805 (2002).
- <sup>21</sup>J. W. P. Hsu, M. J. Manfra, S. N. G. Chu, C. H. Chen, L. N. Pfeiffer, and R. J. Molnar, *Appl. Phys. Lett.* **78**, 3980 (2001).
- <sup>22</sup>J. W. P. Hsu, M. J. Manfra, D. V. Lang, S. Richter, S. N. G. Chu, A. M. Sergeant, R. N. Kleiman, and L. N. Pfeiffer, *Appl. Phys. Lett.* **78**, 1685 (2001).
- <sup>23</sup>F. Iucolano, F. Roccaforte, F. Giannazzo, and V. Raineri, *J. Appl. Phys.* **102**, 113701 (2007).
- <sup>24</sup>B. K. Li, W. K. Ge, J. N. Wang, and K. J. Chen, *Appl. Phys. Lett.* **92**, 082105 (2008).